Geochemistry and petrogenesis of the Permian mafic dykes in the Panxi region, SW China

Jianwei Zi [a,b], Weiming Fan [a,*], Yuejun Wang [a], Touping Peng [a], Feng Guo [a]

[a] *Key Laboratory of Isotope Geochronology and Geochemistry, Guangzhou Institute of Geochemistry, Chinese Academy of Sciences, Guangzhou, 510640, People's Republic of China*
[b] *Graduate School of Chinese Academy of Sciences, Beijing, People's Republic of China*

Abstract

Numerous intrusive bodies of ultramafic–mafic to felsic compositions are exposed in association with volcanic rocks in the Emeishan large igneous province (LIP), southwestern China. In this paper, we present new elemental and isotopic data for the Permian mafic dykes from the Panxi region which is located in the western part of the Emeishan LIP. The characteristics of major and trace elements and Sr–Nd isotopes, in combination with isotopic ages, suggest that these mafic dykes were originated from a similar mantle source related to an upwelling mantle plume and their formation was involved in a process of variable degrees of fractional crystallisation coupled with assimilation of enriched crustal materials. The mafic dyke samples from the Panxi region show some systematic variations in geochemical compositions. The gabbros in Yanyuan contain the lowest REE (e.g., La=5–12 ppm), the highest MgO (8.38–21.33%) and compatible elements (e.g. Cr=104–2610 ppm, Ni=135–496 ppm), and display depleted Sr–Nd isotopic ratios (initial $^{87}Sr/^{86}Sr=0.703752$–0.703844; $\varepsilon_{Nd}(t)=+4.87$ to $+5.13$). These gabbros likely represent an undifferentiated composition similar to primary melts derived from a depleted mantle source. In contrast, the gabbro samples from Panzhihua and Huili have more enriched LREE abundances and incompatible elements, and display depleted to slightly enriched Sr and Nd isotopic signatures (initial $^{87}Sr/^{86}Sr=0.704354$–0.705436; $\varepsilon_{Nd}(t)=-0.29$ to $+4.58$), though their trace element spidergram patterns are similar to those of the Yanyuan samples. These gabbros were formed probably through the removal of a few percent of olivine, clinopyroxene, plagioclase and apatite from the melts that formed the Yanyuan gabbros. All the mafic intrusives in the region exhibit elemental and Sr–Nd isotopic features generally comparable with those of the nearby volcanic rocks. In addition, their emplacement immediately preceded or was synchronous with the main pulse of volcanism that formed lavas over a large area along the western margin of the Yangtze Craton. These lines of evidence suggest that there is a genetic link between the mafic dykes and flood basalts in the Emeishan LIP, and the both share a common mantle source related to the Emeishan plume.

© 2008 International Association for Gondwana Research. Published by Elsevier B.V. All rights reserved.

Keywords: Geochemistry; Emeishan large igneous province; Petrogenesis; Mafic dykes; Panxi region

1. Introduction

The geochemical characteristics of mafic magmatism with respect to the tectonic evolution of the major crustal blocks in China have been investigated in several recent studies (e.g., Peng et al., 2007; Zhou et al., 2007; Hou et al., 2008). The

Emeishan large igneous province (LIP) consists of voluminous outcrops of high- and low-Ti basalts, mafic–ultramafic intrusions and the associated alkaline and felsic rocks in Sichuan, Yunnan, Guizhou, and western Guangxi provinces, SW China (Lin, 1985; Fig. 1). The high- and low-Ti flood basalts are believed to be the products of the Emeishan mantle plume (Chung and Jahn, 1995; Chung et al., 1998; Xu et al., 2001; Zhang et al., 2004), and erupted during the late Permian period (~260 Ma; Yin et al., 1992; Jin and Shang, 2000; Ali et al., 2002; Ali et al., 2004). Similar to the case for the volcanic successions, the associated layered mafic–ultramafic intrusions
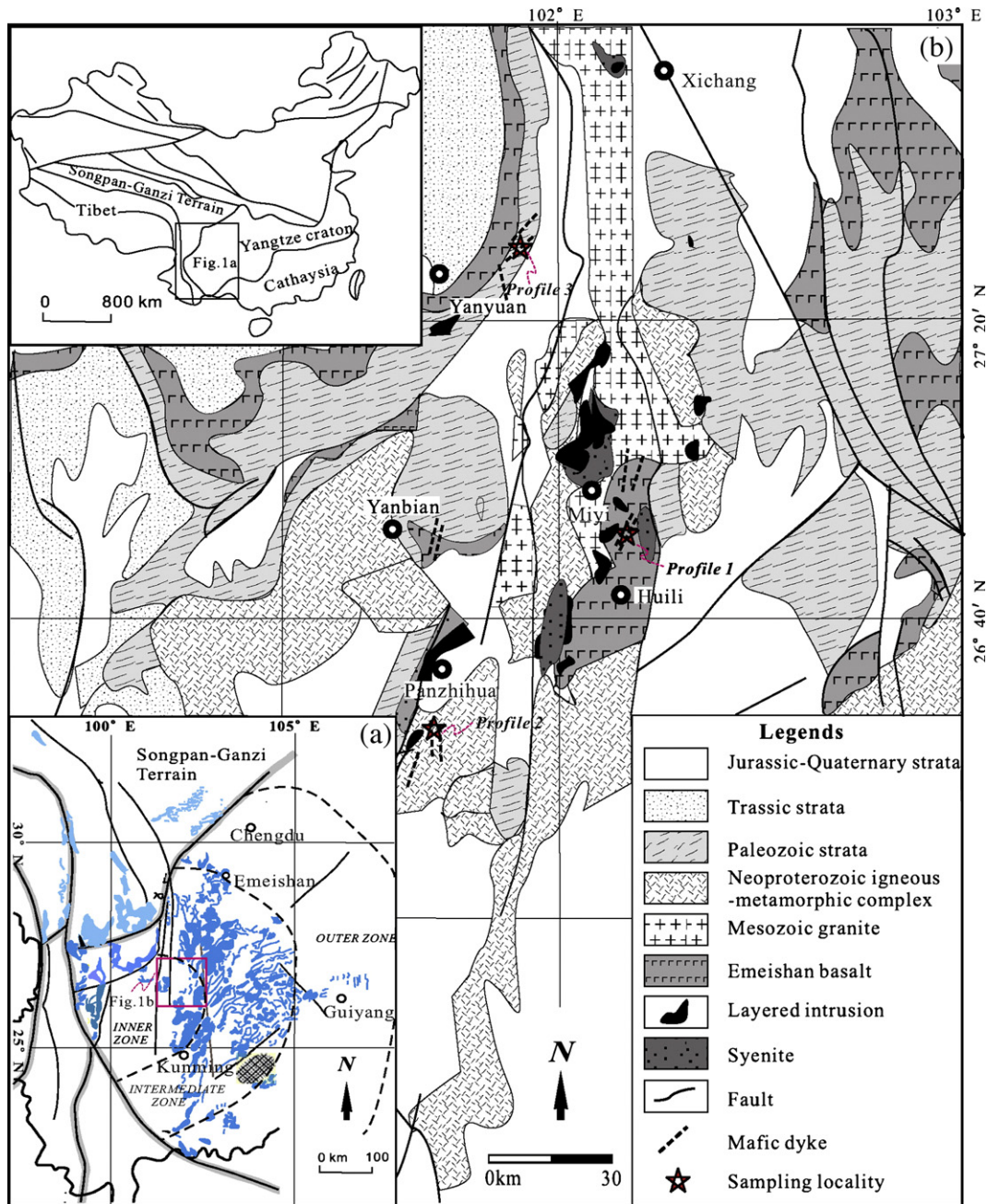
Fig. 1. (a) Distribution of the Emeishan flood basalts and associated intrusions in the Panxi region, SW China; and (b) regional geological map of the studied area (modified after Zhou et al., 2005a).

in the Emeishan LIP have also been paid considerable attention (Luo, 1981; Liu et al., 1985; Zhang et al., 1999) over the past several decades due to the presence of giant Fe–Ti–V deposits in, such as, the Hongge intrusion (PXGT, 1987; Zhong et al., 2002) and the Panzhihua intrusion (Zhou et al., 2005a), and the Cu–Ni–PGE sulfide mineralization in the Yangliuping, Hongge and Xinjie intrusions (Zhong et al., 2003, 2004).

The various rocks in the Emeishan LIP are considered to be associated with variable mantle sources and complex magma processes such as plume–lithosphere interaction and crust contamination (Chung and Jahn, 1995; Song et al., 2001a; Xu et al., 2001; Zhang and Wang, 2002). This is similar to the

hypothesis proposed for rocks in many other LIPs (e.g., Lightfoot et al., 1990, 1993; Arndt and Christensen, 1992; Naldrett et al., 1992; Arndt et al., 1993; Arndt et al., 1998).

In the Panxi (Panzhihua–Xichang) region as well as western Sichuan Province (Fig. 1), there are abundant ultramafic–mafic dykes in association with flood basalts and layered intrusions. Dykes in large igneous provinces are traditionally proposed to be representative of plumbing systems, which presumably fed the lava flows. Therefore, studies of mafic dykes are of great importance for understanding of the plumbing systems, total magma volume and source characteristics of large igneous provinces.

If we can prove that the intrusion of these dykes in the Panxi region was part of the same igneous event that produced the Emeishan LIP, a genetic link between the dykes and the volcanic rocks can then be established. However, previous work paid little attention to these mafic dykes, and in particular, there is a lack of systematic and comparative studies for the region. As such, the petrogenesis and source characteristics of these dykes and their relationship with the large igneous province remain largely unknown. This paper presents a set of new elemental and Sr–Nd isotopic data on the mafic dykes in the Panxi region of the Emeishan LIP. These data, together with the available geochronological results enable us to discuss the nature of the mantle source and magmatic process for the mafic dykes and to advance our understanding of the relationship between the mafic dykes and the Emeishan LIP.

2. Geological background and petrology

Southwest China is an important part of the Yangtze Craton with a Precambrian basement involving Archean crust up to >3.2 Ga (Qiu et al., 2000; Wang et al., 2007). As shown in Fig. 1, it is adjacent to the Songpan–Ganzi Terrain of the Tibetan Plateau in the west. The outcropped stratigraphic sequences in the broad area include Proterozoic clastics, lower Paleozoic marine strata and Devonian to Triassic sediments, and upper Jurassic to Quaternary clastics upwards. Abundant Neoproterozoic granites and associated metamorphic complexes, known as the Kangdian complexes, occur at the western margin of the Yangtze Craton. The biostratigraphic and sedimentologic investigations showed that the western Yangtze Craton underwent a rapid uplift at the end of late Paleozoic due to the impact of the Emeishan mantle plume (He et al., 2003, 2006). During the Cenozoic, thrusting and strike–slip faulting was dominant in this area (Burchfiel et al., 1995).

The Emeishan LIP in Southwest China covers an area of more than 250 000 km^2 near the western margin of the Yangtze Craton. The volcanic succession ranges from several hundred meters up to 5 km in thickness (Chung and Jahn, 1995; Xu et al., 2001) and is composed predominantly of basaltic lavas and pyroclastics. Minor amounts of picrites, basaltic andesites and alkaline rocks also occurred. The volcanic succession is unconformably sandwiched between the underlying Middle Permian Maokou Formation (limestone) and the overlying Late Permian Xuanwei Formation (sandstone and mudstone). In the western part of the Emeishan LIP, the volcanic successions were commonly deformed as the results of the Mesozoic and Cenozoic tectonic events. Previous studies showed that the extensive upper Permian Emeishan LIP was related to a mantle plume system rather than to a rift system (e.g., Chung and Jahn, 1995; Chung et al., 1998; Xu et al., 2001). In the light of the results from magnetobiostratigraphic correlations, the eruption of the Emeishan LIP was traditionally believed to take place in the Late Permian. Recent geochronological data (Zhou et al., 2002; Fan et al., 2004; Shellnutt and Zhou, 2007) gave a more precise dominant eruptive timing of ~260 Ma.

The Emeishan basalts can be divided into low-Ti and high-Ti types. The low-Ti basalts occurred at the lower part and
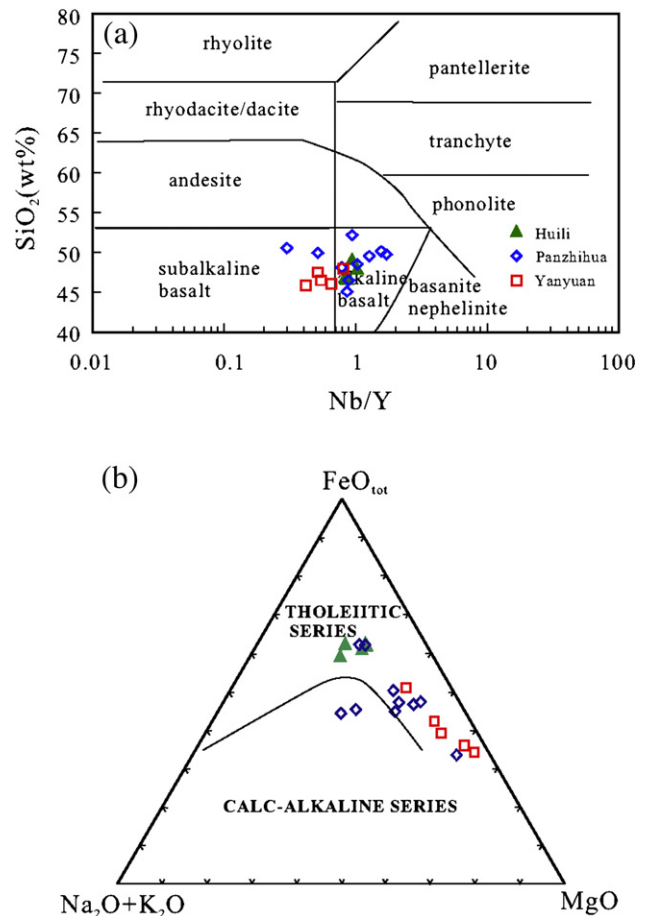

Fig. 2. Plots of the Permian mafic dykes in the Panxi region, SW China. (a) Nb/Y versus SiO$_2$ (after Winchester and Floyd, 1977) and (b) AFM ternary diagram.

the high-Ti lavas are predominant in the upper part of the volcanic succession in the western part of the province. It is generally believed that the high-Ti rocks were formed from relatively lower degree of melting of an inferred plume source with $\varepsilon_{Nd}(t)=+5$ and (^{87}Sr/^{86}Sr)$_i$ ~0.704, whereas the parental magmas of the low-Ti rocks were from higher degree of partial melting (16%) of a distinct mantle source ($\varepsilon_{Nd}(t)$~+2, (^{87}Sr/^{86}Sr)$_i$ ~0.705) (Xu et al., 2001).

The Permian mafic dykes are distributed intermittently along a roughly north–south aligned belt with a length up to hundreds of kilometers (from Lixian in the north to Panzhihua in the south) in western Sichuan province, southwestern China (Fig. 1). The Panxi region (also named the Panxi paleorift by Chinese geologists) is a roughly north–south trending zone in the central part of the Emeishan LIP along the western margin of the Yangtze Craton (Fig. 1b). The mafic dykes examined in this study are exposed predominantly within this zone. These dykes have variable strikes of 340°, 40° and 290°, mostly having steep E- to NE dips of ~70°. All these dykes in the Panxi region are located in the inner zone of the Emeishan LIP defined by He et al. (2003) (see Fig. 1a). The width of a single dyke ranges from less than 1 m to dozens of meters, and the length ranges from ~10 m to hundreds of meters. These dykes are predominantly of mafic compositions (with small amounts of ultramafic rocks and syneites), and they always occur in

Table 1
Major and trace element abundances of the late Permian mafic dykes in Panxi region, SW China

Sample #	SCHL-2	SCHL-4	SCHL-6	SCHL-7	SCHL-10	SCHL-45	SCHL-48	SCHL-50	SCHL-53	SCHL-54	SCHL-55	SCHL-57	SCHL-58	SCHL-63	SCHL-64	SCHL-65	SCHL-67	SCHL-68	SCHL-69	SCHL-70
Location	Huili					Panzhihua										Yanyuan*				
Major elements (%)																				
SiO_2	46.3	45.9	46.8	48.2	46.0	48.4	49.8	47.2	43.8	48.5	49.1	48.3	47.1	49.6	45.6	45.4	46.3	45.6	45.3	47.1
TiO_2	3.30	3.64	4.09	3.37	3.61	2.15	0.79	2.09	1.50	2.40	1.82	2.62	2.08	1.02	3.83	1.08	1.46	1.75	1.04	1.69
Al_2O_3	13.4	12.7	12.7	13.1	12.6	12.0	17.6	11.7	7.97	10.5	13.0	11.6	11.3	13.6	12.6	6.35	15.7	10.2	5.80	8.66
Fe_2O_3	4.89	3.37	3.96	3.52	4.55	3.49	0.72	3.90	3.50	4.14	4.37	4.60	3.39	2.09	4.33	1.57	3.35	3.14	1.96	3.23
FeO	10.1	12.2	11.7	10.7	11.1	8.83	7.4	7.95	8.52	7.57	10.4	6.93	8.23	7.17	11.3	10.8	7.83	7.97	9.63	6.63
CaO	10.2	10.3	8.44	8.73	10.5	10.6	11.9	11.5	8.34	10.1	10.3	9.40	11.4	9.49	10.1	10.9	11.6	14.2	12.3	15.1
MgO	5.78	5.85	4.83	4.68	5.99	8.73	7.08	10.6	20.7	9.62	5.66	7.38	10.6	5.44	5.72	20.3	8.38	12.8	21.3	13.1
MnO	0.23	0.24	0.26	0.21	0.24	0.20	0.15	0.18	0.17	0.16	0.24	0.14	0.17	0.18	0.23	0.20	0.17	0.16	0.19	0.16
K_2O	0.76	0.77	1.35	1.39	0.54	0.94	0.73	0.57	1.36	1.92	0.69	5.09	0.76	0.48	0.90	0.22	0.41	0.17	0.14	0.28
Na_2O	2.73	2.44	3.01	3.37	2.67	2.16	2.02	1.99	1.14	1.47	2.45	0.61	1.48	5.38	2.72	1.28	1.75	1.84	0.85	1.76
P_2O_5	0.31	0.33	0.44	0.41	0.30	0.24	0.17	0.22	0.13	0.30	0.20	0.32	0.25	0.53	0.28	0.11	0.12	0.11	0.06	0.14
LOI	1.79	2.04	2.13	2.03	1.61	1.98	1.44	1.83	3.49	2.99	1.56	2.64	3.00	4.80	2.11	1.49	2.64	1.85	1.18	1.87
Mg#	0.43	0.41	0.37	0.38	0.42	0.57	0.61	0.63	0.77	0.61	0.42	0.55	0.63	0.52	0.41	0.75	0.59	0.69	0.77	0.72
Trace elements (ppm)																				
Cr	31.9	26.2	12.5	17.2	37.1	221	237	711	1520	587	42.9	447	604	106	22.5	1220	104	862	2611	1763
Ni	64.0	61.5	40.9	44.2	64.7	121	17.9	210	902	162	51.9	121	261	46.7	61.2	486	135	206	496	297
Rb	22.8	26.0	39.4	43.7	14.5	39.0	27.1	13.9	12.2	47.5	30.7	164	27.4	7.14	26.7	4.88	11.1	2.36	3.10	8.10
Sr	460	460	370	437	421	485	340	386	254	720	378	976	341	394	405	159	277	254	128	267
Y	30.1	32.5	38.9	34.7	29.3	22.9	20.8	22.1	14.7	22.8	32.4	22.7	23.2	20.2	26.1	13.0	16.4	18.4	12.5	17.3
Zr	197	185	277	233	180	179	42.9	135	98.4	243	111	254	132	122	172	62.1	71.9	75.6	46.5	92.3
Nb	25.8	27.1	39.8	32.1	24.6	28.9	6.22	17.2	12.5	35.5	16.5	38.0	23.5	18.7	22.8	8.47	8.25	9.98	5.16	13.9
Cs	0.49	1.22	0.71	0.57	0.43	1.12	0.29	0.24	1.35	0.16	0.55	0.30	0.14	0.09	0.42	0.10	1.71	0.09	0.24	0.39
Ba	368	393	510	529	287	373	203	195	125	490	259	725	461	192	329	86.4	99.0	90.5	66.1	217
La	28.1	28.2	35.9	36.0	25.7	32.5	13.6	17.4	12.2	39.0	15.3	42.5	17.8	17.7	24.2	7.45	7.68	8.36	4.79	11.8
Ce	59.9	61.1	75.6	73.9	56.1	70.0	32.0	40.6	29.0	90.3	33.7	91.0	40.7	35.5	53.1	17.2	18.7	21.4	12.5	28.2
Pr	7.85	8.13	10.1	9.45	7.61	8.26	3.98	5.02	3.64	11.0	4.32	11.2	5.11	3.91	6.76	2.39	2.42	3.03	1.83	3.90
Nd	33.8	36.6	44.8	43.0	32.8	33.1	16.6	22.6	16.3	46.2	18.7	47.5	23.0	15.6	28.7	10.8	11.5	14.4	8.96	17.8
Sm	7.52	8.03	10.4	9.51	7.43	6.91	3.52	5.75	3.81	9.50	4.47	9.25	5.81	3.50	6.56	2.97	3.33	4.24	2.64	4.46
Eu	2.31	2.34	2.43	2.76	2.29	1.92	1.13	1.58	1.09	2.46	1.44	2.43	1.56	0.88	2.06	0.89	1.06	1.22	0.80	1.31
Gd	7.35	7.76	8.26	8.50	7.23	5.71	3.62	4.91	3.54	7.32	5.39	7.34	5.38	3.57	6.30	2.85	3.27	4.16	2.78	4.44
Tb	1.08	1.17	1.23	1.29	1.04	0.82	0.62	0.78	0.55	1.02	0.95	0.96	0.83	0.58	0.92	0.44	0.56	0.62	0.45	0.67
Dy	5.98	6.76	7.41	7.47	5.72	4.56	3.90	4.71	3.21	5.09	5.77	4.95	4.74	3.73	5.42	2.63	3.17	3.96	2.46	3.86
Ho	1.17	1.19	1.35	1.29	1.19	0.82	0.72	0.86	0.58	0.88	1.20	0.89	0.86	0.74	1.02	0.52	0.63	0.70	0.49	0.69
Er	2.94	3.32	3.82	3.59	2.97	2.35	2.20	2.16	1.58	2.40	3.62	2.34	2.32	2.28	2.54	1.24	1.79	1.82	1.29	1.78
Tm	0.42	0.45	0.54	0.49	0.40	0.29	0.33	0.31	0.21	0.33	0.58	0.29	0.34	0.31	0.39	0.20	0.21	0.26	0.18	0.23
Yb	2.48	2.59	3.32	3.05	2.55	1.94	1.90	1.95	1.22	1.89	3.35	1.86	1.87	2.04	2.29	1.16	1.48	1.40	1.05	1.43
Lu	0.34	0.40	0.47	0.45	0.36	0.24	0.27	0.27	0.18	0.24	0.51	0.25	0.27	0.32	0.32	0.16	0.21	0.19	0.15	0.20
Hf	5.84	5.55	6.49	6.89	5.68	5.27	1.54	4.09	3.12	7.35	3.64	7.60	4.23	3.70	5.26	2.09	2.32	2.88	1.88	3.22
Ta	1.60	1.73	1.94	2.03	1.59	1.70	0.30	0.98	0.81	2.16	0.91	2.28	1.96	1.05	1.43	0.49	0.51	0.62	0.34	0.86
Pb	3.58	3.98	3.65	4.75	4.05	4.36	3.44	2.56	1.67	8.15	2.90	4.78	2.60	4.67	3.53	2.00	2.19	1.42	1.75	2.20
Th	3.59	3.38	5.14	4.61	3.50	4.13	0.89	1.89	1.62	5.66	2.39	5.62	2.27	6.31	3.19	0.75	0.67	0.75	0.49	1.21
U	0.84	0.76	1.07	1.10	0.76	0.90	0.20	0.45	0.37	1.22	0.52	1.21	0.55	1.09	0.75	0.22	0.19	0.12	0.12	0.28

LOI, loss on ignition. Mg#=$Mg^{2+}/(Mg^{2+}+Fe^{2+})$ in atomic ratio, assuming Fe^{2+} is 89% total iron and total iron as FeOt. *Data of Yanyuan samples are from Guo et al. (2004).

association with the flood basalts (SBGMR, 1991). The host rocks of these mafic dykes vary throughout the Panxi region. For instance, the dykes seen in the Huili and Panzhihua areas emplaced into Permian flood basalts or Neoproterozoic granites, whereas those in the Yanyuan area intruded into Lower Devonian limestones (Fig. 2).

The rock samples collected and analyzed in this study include olivine-bearing gabbros, gabbros and diabases containing the mineral assemblage of olivine (3–10%), orthopyroxene (5–15%), clinopyroxene (30–45%), plagioclase (30–40%), and accessory ilmenite, magnetite, zircon, and apatite. Zones of olivine cumulate enrichment are observed in the sample from the Yanyuan area, which is indicative of significant crystal fractionation.

3. Analytical techniques

Major oxide compositions were analyzed at the Hubei Institute of Geology and Mineral Resources, the Ministry of Land and Resources, employing wavelength X-ray fluorescence spectrometry (XRF) with analytical errors <2%. Trace element ICP-MS analysis was carried out at the Institute of Geochemistry, the Chinese Academy of Sciences (CAS). Detailed descriptions of the analytical technique and analytical errors can be found in Qi et al. (2000). Sr and Nd isotopic ratios were measured at the Institute of Geology and Geophysics, the CAS. Rock chips <20 mesh grain size were used for Sr and Nd isotope analyses. Before being grounded to <160 mesh and subjected to chemical dissolution, these chips was leached by purified 6 N HCl for 24 h at room temperatures to remove the influence of surface alteration or weathering. The Sr and Nd isotopic ratios were normalized to $^{86}Sr/^{88}Sr = 0.1194$ and $^{146}Nd/^{144}Nd = 0.7219$, respectively. The La Jolla standard yielded $^{143}Nd/^{144}Nd = 0.511862 \pm 12$ ($n = 10$) and the NBS987 standard gave $^{87}Sr/^{86}Sr = 0.710240 \pm 10$ ($n = 6$). The whole procedure blank ranges from 2 to 5×10^{-10} g for Sr and less than 5×10^{-11} g for Nd. The analytical errors for Sr and Nd isotopic ratios are given as 2σ.

4. Results

4.1. Bulk-rock geochemical data

Major and trace element data for representative samples from the Panxi region are presented in Table 1. These Permian mafic rocks plot in the subalkaline- and alkalie-basalt fields on a SiO_2 versus Nb/Y classification diagram (Fig. 2a). The analyzed samples are generally fresh as reflected by small loss-on-ignition (LOI) values (Table 1) and good correlation between Th, U, Rb, Ba, Sr, Pb, Nd, La, Nb and Zr (Fig. 3). Moreover, the Nb/La and Th/La ratios exhibit an insignificant correlation with LOI and Eu/Eu*, respectively. These features suggest that most highly incompatible elements were only slightly affected by post-magmatic processes (Table 1). On an AFM diagram, all the samples define a tholeiitic evolving trend (Fig. 2b).

The gabbroic rocks from Huili have relatively low Mg# (0.38–0.43), Cr (12.5–37.1 ppm) and Ni (40.8–64.7 ppm) con-

tents, but have elevated FeO_t (13.90–15.29 wt.%, average 14.82 wt.%) and TiO_2 (3.30–4.09 wt.%, average 3.60 wt.%) over a range of MgO from 4.68 to 5.99 wt.%. The samples from Panzhihua have moderate Mg# (0.42–0.63, average 0.55) and MgO (5.44–10.60 wt.%, average 7.87 wt.%) except for the sample of SCHL-53 (Mg#=0.77 and MgO=20.68 wt.%). Their Cr and Ni concentrations range from 22.5 to 710.8 ppm and from 17.9 to 210.3 ppm, respectively. The samples from Yanyuan span a relatively narrow variation in SiO_2 (45.28–47.08 wt.%, average 45.93 wt.%) and TiO_2 (1.04–1.75 wt.%, average 1.40 wt.%) contents. They have higher Mg# (0.59–0.77, average 0.70), MgO (8.38–21.33 wt.%, average 15.17 wt.%) and Cr (104.2–2610.8 ppm) and Ni (135.2–495.5 ppm) concentrations relative to those from Huili and Panzhihua.

These mafic samples generally display coherent variation trends in the plots of SiO_2 and major oxides (Fig. 4), indicating a significant crystallizational differentiation for these intrusive rocks. MgO, FeO_t, TiO_2 concentrations and CaO/Al_2O_3 ratio negatively correlate with SiO_2, whereas K_2O and Al_2O_3 positively correlate with SiO_2 (Fig. 4a–h). Cr and Ni contents show a positive correlation with MgO (Fig. 5a–b). In addition, a weak correlation between Sr and MgO is also observed (not shown).

In the chondrite-normalized REE patterns (Fig. 6a–c), all these samples exhibit more enrichment in LREE relative to HREE. As shown in Fig. 6, the samples from Yanyuan have the lowest REE contents (ΣREE=40.3–80.8 ppm, average 58.8 ppm) and LREE/HREE ratios (e.g., La/Yb$_{CN}$=3.29–5.92, average 4.36) in comparison with those from the Panzhihua and Huili areas. Furthermore, the sample from Yanyuan shows an insignificant LREE fractionation with the La/Sm$_{CN}$ ratio ranging from 1.17 to 1.71 (average 1.45). Also shown in Fig. 6a–c are slightly negative Eu anomalies (Eu/Eu*=0.78–0.97) for all the samples from the areas. On primitive mantle-normalized trace element spidergrams (Fig. 6d–e), these samples show the trace element patterns similar to that for OIB, with the exception of prominent negative P anomaly and slightly positive Ti anomaly. It is also noted that the spidergram for the Yanyuan samples shows marked Th–U depletion relative to Nb–Ta, in clear contrast to those for the Huili and Panzhihua samples (Fig. 3d–e).

As described above, the less evolved samples with Mg#> 0.75 (e.g., SCHL-53 from Panzhihua and SCHL-65 and SCHL-69 from Yanyuan) have higher MgO, Ni and Cr contents (Table 1) than those of the more evolved samples. These rocks may reflect the result of olivine and/or clinopyroxene cumulus, consistent with petrological observations.

4.2. Sr–Nd isotopic compositions

Sr and Nd isotopic data for selected samples are presented in Table 2. The initial Sr and Nd isotopic ratios have been corrected using the formation age of 260 Ma. The samples from Huili and Panzhihua have initial $^{87}Sr/^{86}Sr$ ratios ranging from 0.704354 to 0.705436 and age-corrected $\varepsilon_{Nd}(t)$ values from −0.29 to +4.58. In contrast, the representative samples from Yanyuan have the initial $^{87}Sr/^{86}Sr$ ratios of 0.703752–0.703844,
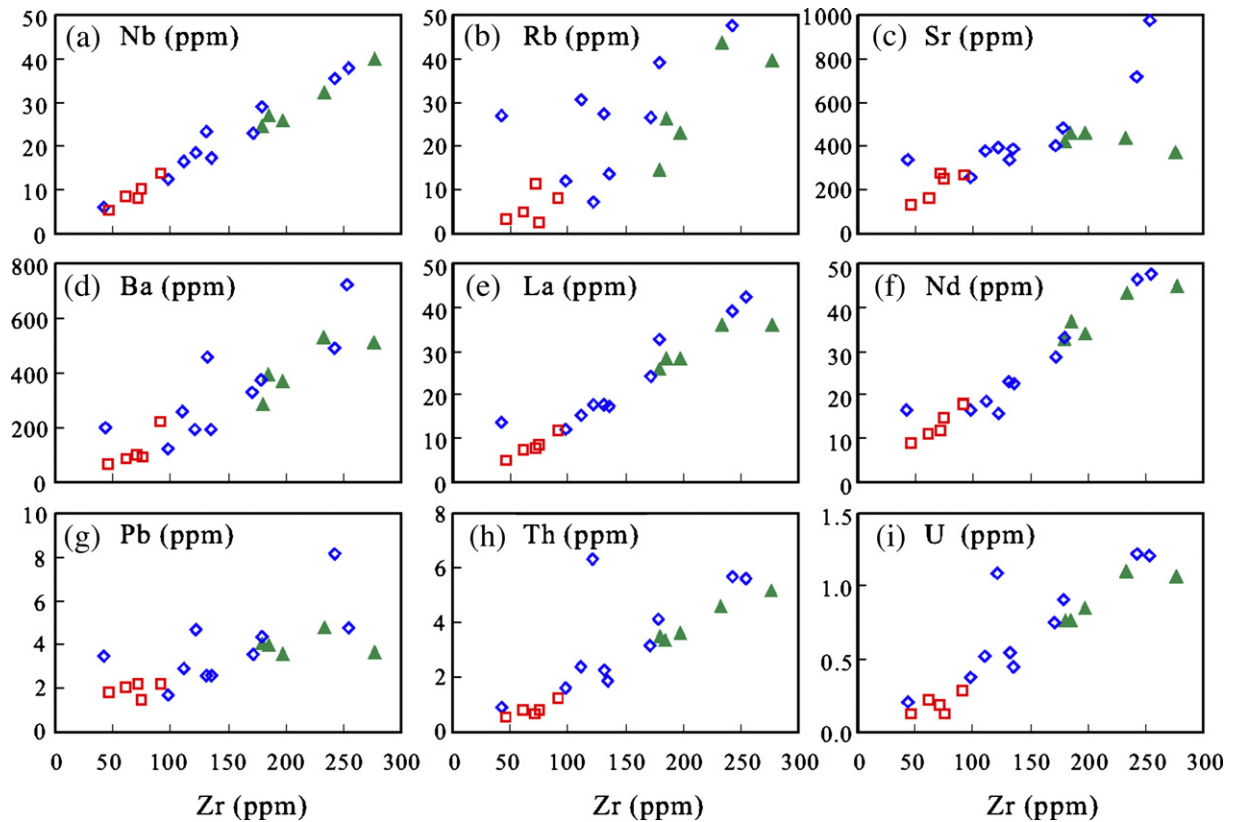
Fig. 3. Variations of selected incompatible elements versus Zr for the Permian mafic dykes in the Panxi region, SW China. Symbols are the same as those in Fig. 2a.

and $\varepsilon_{Nd}(t)$ values of +4.87 to +5.13 (Table 2). The variations in the isotopic compositions of the samples from all the three areas may reflect the source heterogeneity or different magma process. In the plot of $(^{87}Sr/^{86}Sr)_i$ versus $\varepsilon_{Nd}(t)$ value, all the samples are plotted in the field defined by the Emeishan flood basalts with an affinity to the OIB-type source. A significantly negative correlation between $\varepsilon_{Nd}(t)$ values and $(^{87}Sr/^{86}Sr)_i$ ratios can be recognized (Fig. 7).

5. Discussion

5.1. Emplacement age of the mafic dykes

Previous geochronological data for the Emeishan flood basalts are dominantly represented by the $^{40}Ar/^{39}Ar$ plateau ages of <256 Ma (e.g., Boven et al., 2002; Lo et al., 2002; Ali et al., 2004; Fan et al., 2004). More recent SHRIMP zircon U–Pb results for the basalts, mafic–ultramafic to felsic intrusions and silicic ignimbrites from the Emeishan LIP have defined a consistent crystallization age at ~260 Ma (e.g., Zhou et al., 2002, 2005a; Luo et al., 2007; Zhong et al., 2007; Fan et al., in press). For example, two representative basalts in western Guangxi Province with geochemical affinities to the Emeishan LIP gave the SHRIMP U–Pb zircon ages of 259.6±5.9 Ma and 259.1±4.0 Ma, respectively (Fan et al., in press), and the flood basalts in the Songpan–Ganzi region also gave a SHRIMP zircon U–Pb age of ~260 Ma (the authors' unpublished data). These ages represent the eruption time of these lavas.

Ultramafic rocks from Xinjie (the Panxi region), the mafic intrusions in Anding (southeastern Yunnan province) and the diabasic sills in Shadou (eastern Yunnan) are geochemically similar to the Emeishan low-Ti basalts, which yielded the weighted mean $^{206}Pb/^{238}U$ ages of 259±3 Ma, 258±3 Ma, 260±3 Ma, respectively (Zhou et al., 2002, 2005a,b). The mafic dyke samples collected from Yanyuan in the Panxi region gave a weighted mean $^{206}Pb/^{238}U$ ages of 262±3 Ma (Guo et al., 2004). Moreover, a syenite that is spatially associated with the mafic dykes in the Emeishan LIP also has the formation age of 261.6±4.4 Ma (Luo et al., 2007). All these dating data define a rather consistent age range. However, Shellnutt et al. (in press) recently reported a zircon U–Pb age of ~242 Ma for a mafic dyke in the Panxi region, and considered this magmatic pulse occurred at about 18 Ma after the main magmatism of the Emeishan plume. This speculation is based on very limited data and needs to be validated through further detailed work. In summary, based on our geological observations and, geochemical characteristics, together with the bulk SHRIMP zircon dating data (e.g., the age for the Yanyuan dyke), we would like to propose that all the mafic dykes involved in the study area were emplaced around 260 Ma, which was contemporaneous with the eruption of the aforementioned flood basalts and the emplacement of the adjacent mafic–ultramafic layered intrusions associated with the Emeishan LIP. Therefore, the intrusion of these mafic dykes in the Panxi region was part of the major magmatic event for the Emeishan LIP.
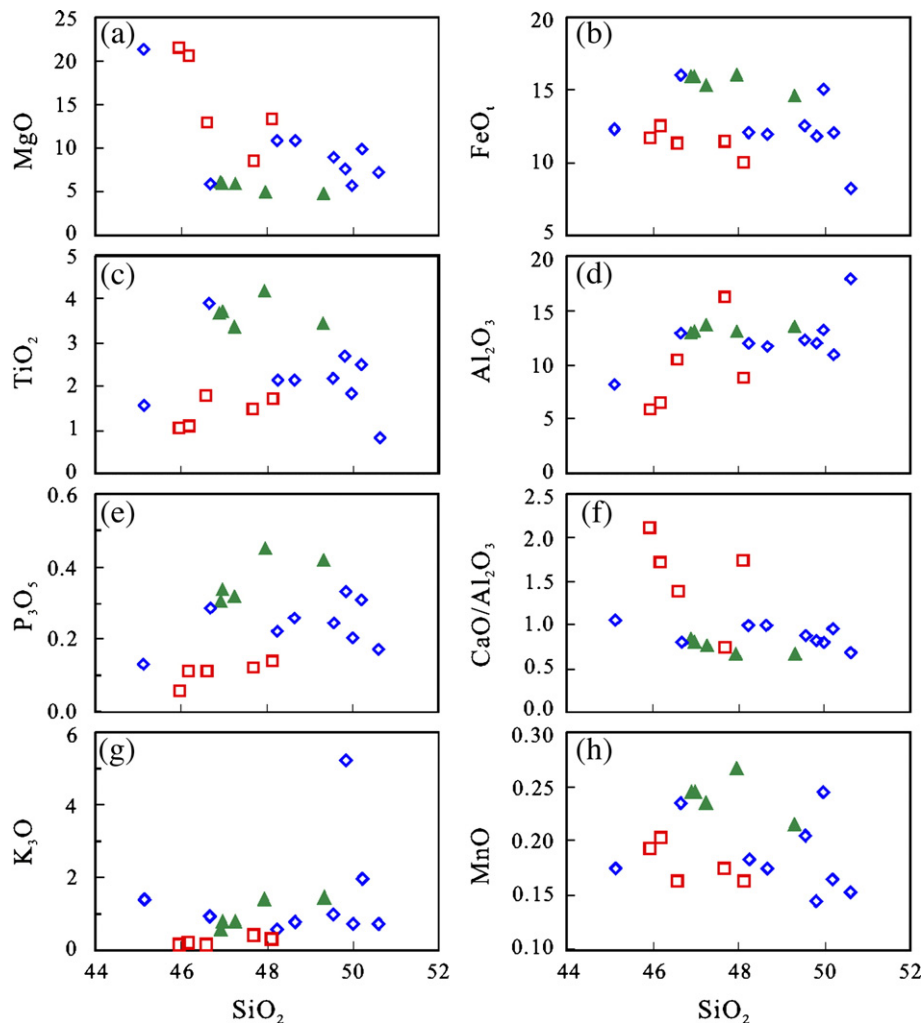
Fig. 4. Variations of oxides versus SiO$_2$ for the Permian mafic dykes in the Panxi region, SW China. Symbols are the same as those in Fig. 2a.

5.2. Petrogenesis

5.2.1. Magma processes

The wide ranges of Mg#, MgO, Ni and other compatible element contents (Table 1) indicate that the Permian mafic dykes in the Panxi region underwent extensive crystallization fractionation either in magma chambers or during ascent. Such a crystallization fractionation is also evidenced by the regular variations of other elemental concentrations.

The decreases in MgO and FeO$_t$ contents with an increase in SiO$_2$ (Fig. 4a, b) indicate the crystallization fractionation of olivine. The negative correlation between SiO$_2$ and CaO/Al$_2$O$_3$ (Fig. 4f) suggests the involvement of clinopyroxene fractionation. The decrease of compatible elements (e.g., Cr and Ni) with magma evolution (Fig. 5a–b) also supports the occurrence of the fractionation crystallization of olivine and clinopyroxene, compatible with the presence of olivine and clinopyroxene cumulus for these rocks (Fig. 8). The pronounced depletion of P in Fig. 3d–f may be related to the crystallization fractionation of apatite. This is also supported by the correlation between P$_2$O$_5$ and La (Fig. 4j). A proportional fractionation of plagioclase can account for the negative Sr and Eu anomalies (Eu/Eu*=0.78–

0.94; see Fig. 3a, d) displayed by the samples from Huili. A negative correlation between Ti, Fe and SiO$_2$ (Fig. 4b, c) for the samples from Panzhihua could be related to the crystallizational fractionation of Fe–Ti oxides. This consideration is in agreement with the occurrence of giant Fe–Ti–V oxides deposits in this region (e.g., Zhou et al., 2005a). In contrast to the features described above, the samples from Yanyuan have the highest compatible element contents (e.g., MgO, Ni and Cr contents) among all the analysed samples. This suggests that the dykes in Yanyuan may be more primary relative to those from Huili and Panzhihua.

In summary, our analyses suggest that all the dykes in our study areas in the Panxi region experienced various degrees of the crystallizational fractionation of olivine and clinopyroxene, as well as plagioclase, apitite and titanomagnetite. During the evolutions of the mafic dykes, mafic minerals (e.g., olivine and clinopyroxene) were predominant in the earlier melts, whereas felsic minerals (e.g., plagioclase) were abundant in the later melts of the magma.

Our data imply the involvement of extensive crystallization fractionation during the emplacement of magmas, and an increase in SiO$_2$ with the decrease of MgO likely indicates the
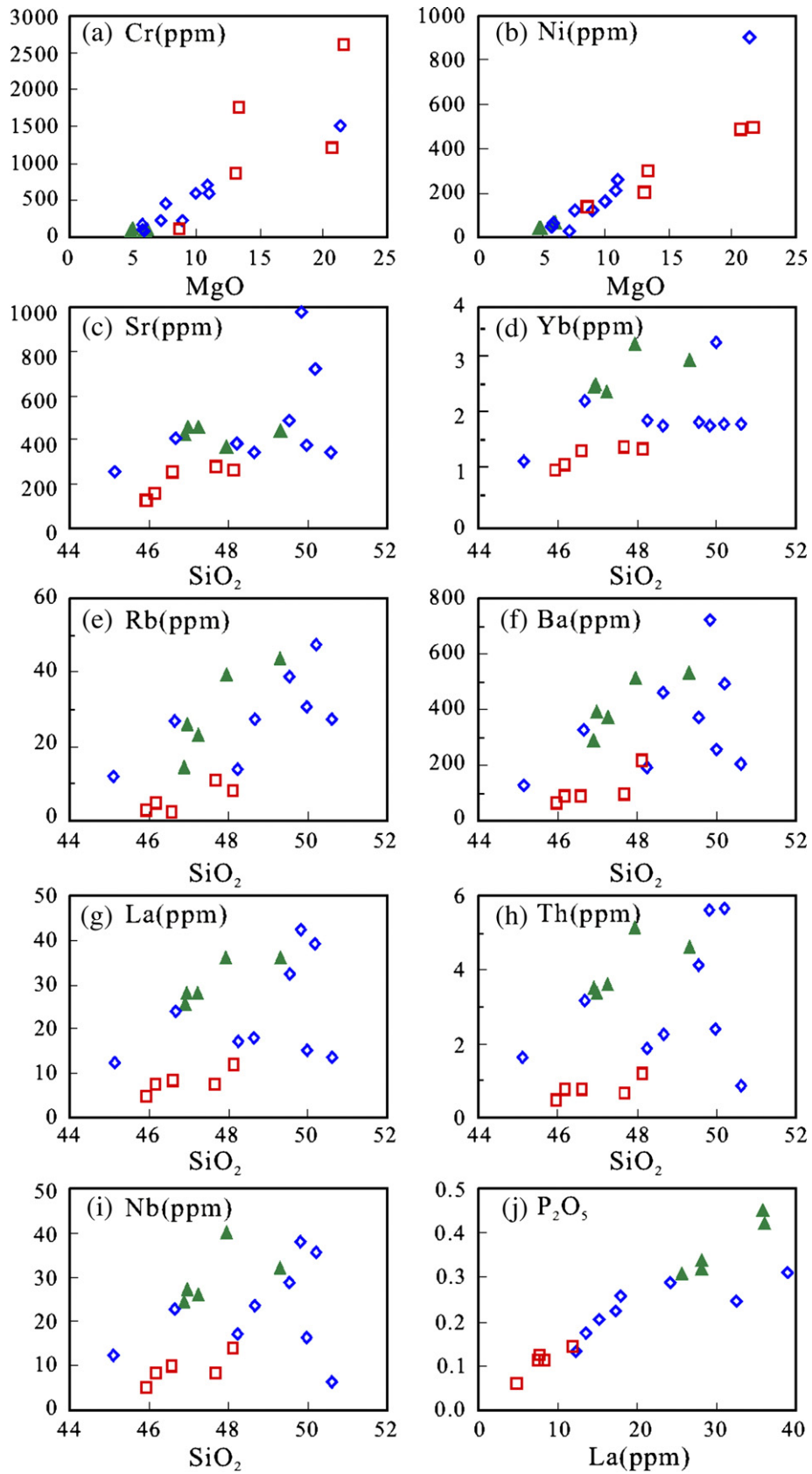
Fig. 5. Variations of Ni, Cr versus MgO (a–b) and Sr, Yb, Rb, Ba, La, Th, Nb versus SiO$_2$ (c–i) and, P$_2$O$_5$ versus La (j) for the Permian mafic dykes in the Panxi region, SW China. Symbols are the same as those in Fig. 2a.
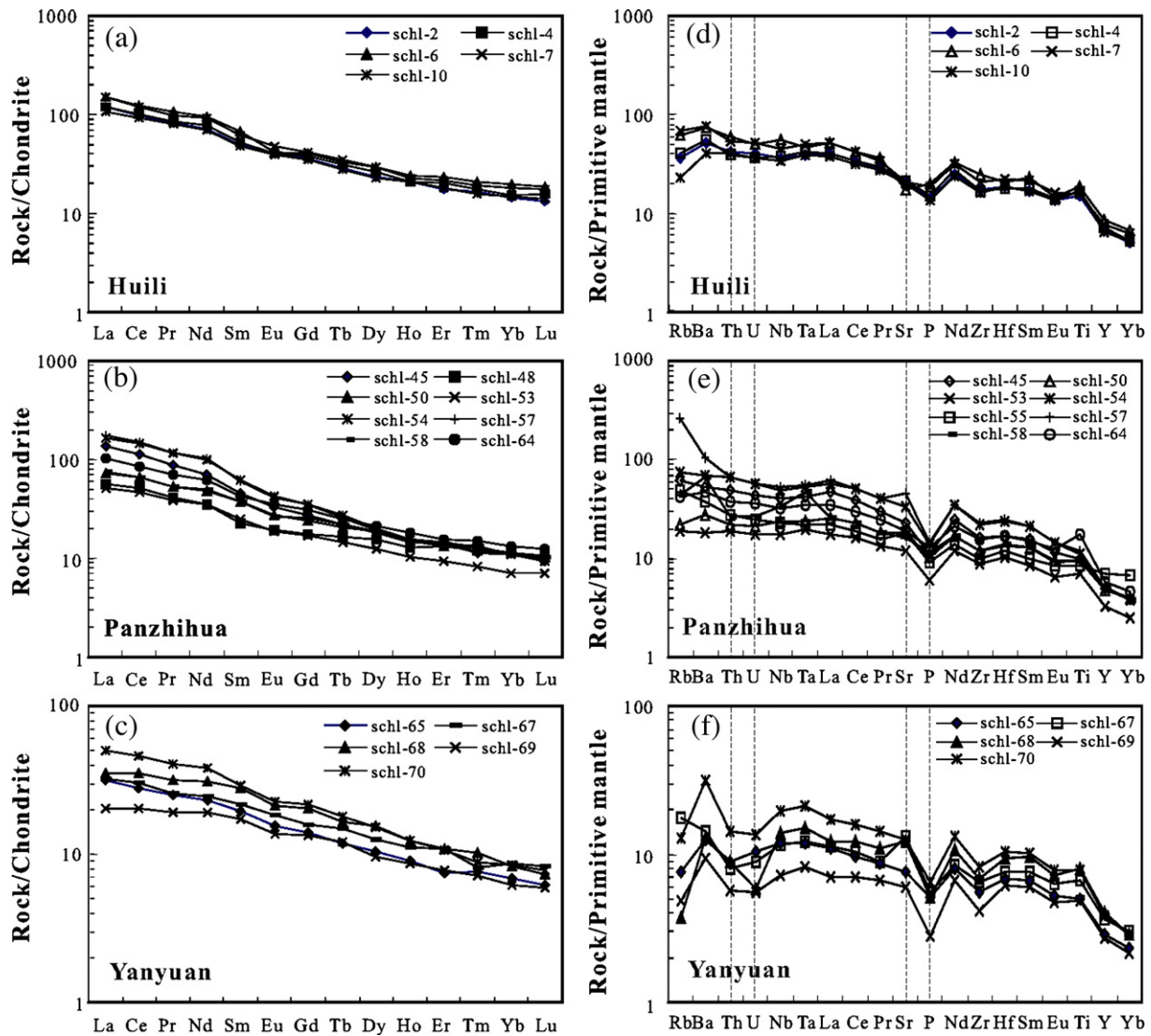
Fig. 6. Chondrite-normalized REE patterns (a–c) and primitive mantle-normalized spidergrams (e–f) for the late Permian mafic dykes in the Panxi region, SW China. Normalization values for chondrite and primitive mantle are from Taylor and McLennan (1985) and Sun and McDonough (1989), respectively.

input of crustal materials. The scatter of both $(^{87}Sr/^{86}Sr)_i$ and $\varepsilon_{Nd}(t)$ values of these samples is in accordance with variable degrees of crustal contamination (Fig. 7). The samples with

relatively higher $(^{87}Sr/^{86}Sr)_i$ ratios and lower $\varepsilon_{Nd}(t)$ values generally have higher SiO_2 contents and Th/Nb ratios, and this warrants the speculation of the involvement of an assimilation

Table 2
Sr and Nd isotope data for the late Permian mafic dykes in Panxi region, SW China

| Sample #	Sm (ppm)	Nd (ppm)	Rb (ppm)	Sr (ppm)	$^{147}Sm/^{144}Nd$	$^{143}Nd/^{144}Nd \pm 2\sigma$	$^{87}Rb/^{86}Sr$	$^{87}Sr/^{86}Sr \pm 2\sigma$	$^{87}Sr/^{86}Sr(i)$	$\varepsilon_{Nd}(t)$
Huili										
SCHL-2	7.52	33.8	22.8	460	0.134406	0.512639±10	0.143790	0.705525±19	0.704993	2.09
SCHL-4	8.03	36.6	26.0	460	0.132918	0.512667±9	0.163995	0.704961±20	0.704354	2.68
SCHL-10	7.43	32.8	14.5	421	0.137062	0.512667±10	0.099767	0.705805±19	0.705436	2.55
SCHL-15	5.83	29.8	91.1	552	0.118139	0.512517±10	0.47867	0.706880±20	0.705109	0.25
SCHL-24	5.2	27.5	105	568	0.114351	0.512397±7	0.533715	0.707590±20	0.705616	−1.97
Panzhihua										
SCHL-45	6.91	33.1	39.0	485	0.126154	0.512503±8	0.232965	0.706166±21	0.705304	−0.29
SCHL-50	5.75	22.6	13.9	386	0.153972	0.512637±10	0.104116	0.704915±18	0.704530	1.40
SCHL-53	3.81	16.3	12.2	254	0.141104	0.512778±8	0.139457	0.704901±19	0.704385	4.58
Yanyuan										
SCHL-65	2.97	10.8	4.88	160	0.165687	0.512848±8	0.088674	0.704080±21	0.703752	5.13
SCHL-70	4.46	17.8	8.10	267	0.151183	0.512810±12	0.087960	0.704169±19	0.703844	4.87
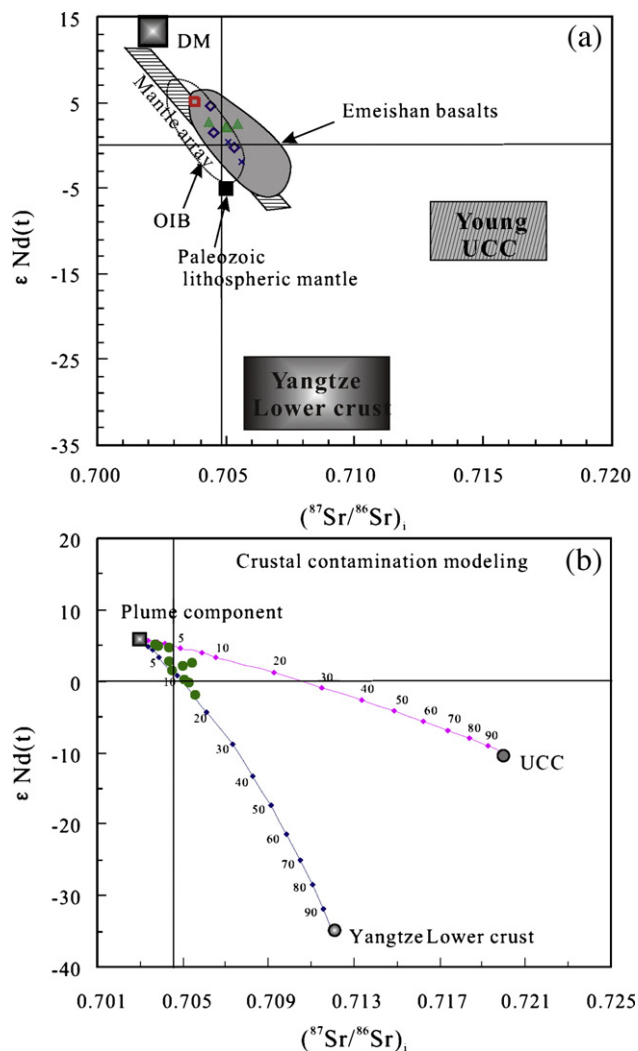
Fig. 7. (a) $\varepsilon_{Nd}(t)$ vs. initial $^{87}Sr/^{86}Sr$ plot (t=260 Ma) for the Permian mafic dykes in the Panxi region, SW China. The field of the Emeishan basalts is after Xu et al. (2001). The Yangtze lower crust represented by the Kongling granitic gneiss is after (Gao et al., 1999; Ma et al., 2000), upper crust (UC) are from Rudnick and Gao (2003). Other fields are from literature data. (b) The contamination curves for source and crustal materials. Symbols are the same as those in Fig. 2a.

and fractional crystallization (AFC) (Fig. 9). The AFC process is commonly utilized to explain the geochemical differences between continental flood basalts and ocean island basalts or mid-ocean-ridge basalts (e.g., Mahoney, 1988; Arndt et al., 1993). According to the hypothesis of DePaolo (1981), AFC could result in the significant increase of $(^{87}Sr/^{86}Sr)_i$ and decrease of $\varepsilon_{Nd}(t)$ values with the increase of SiO_2. Such characteristics can be observed in our samples (Fig. 9a–c, e). In addition, the large scatter of MgO, Ni and Cr contents and the correlation between $\varepsilon_{Nd}(t)$ and $^{147}Sm/^{144}Nd$ (Fig. 9d), $(^{87}Sr/^{86}Sr)_i$ and 1/Sr (Fig. 9f) are also observed. Therefore, we propose that the AFC process was involved during the evolution of magmas in the region.

5.2.2. Nature of source: mantle plume-derived melts

It has been well documented that the Emeishan flood basalts were derived from a mantle plume source contaminated by an enriched lithospheric component (Chung and Jahn, 1995; Song et al., 2001b; Xu et al., 2001).

The high $\varepsilon_{Nd}(t)$ and low $(^{87}Sr/^{86}Sr)_i$ arrays defined by the samples from Yanyuan (see Fig. 7) indicate a mantle source that is isotopically identical to the least contaminated picrites in the Emeishan LIP (Chung and Jahn, 1995; Zhang et al., 2006) and also similar to those of oceanic hotspots (calculated to 260 Ma). Moreover, the multi-element and REE patterns (Fig. 6) as well as incompatible element ratios (Fig. 9) of these mafic intrusives are similar to those of the Emeishan picrites, suggesting an OIB-type mantle source. Although such geochemical signatures may also be compatible with processes other than the mantle plume model (e.g., Sheth, 2005), the combination of the OIB-type geochemical and isotopic features, together with anomalously high temperatures (1500–1550 °C, Xu et al., 2001; 1630–1690 °C, Zhang et al., 2006) and large pre-volcanic regional lithospheric uplift/doming (He et al., 2003; Xu et al., 2004; He et al., 2006), suggests that a mantle plume origin model is more likely.

Zr/Nb and Ce/Y ratios are in the range of 5.61–9.02 and 1.00–4.01, respectively. In the Zr/Nb and Ce/Y diagram proposed by Deniel (1998), the studied mafic rocks plot in the field of the melting column across the garnet–spinel lherzolite transition. In particular, the samples from Yanyuan are characterized by high compatible element abundances and $\varepsilon_{Nd}(t)$ values (4.87 to 5.13) and low $(^{87}Sr/^{86}Sr)_i$ ratios (0.703752 to 0.703844), as well as depletion of Th and U relative to neighbor elements (e.g., Ba, Nb and Ta) (Fig. 6f). These likely represent the geochemical and isotopic signatures of the Emeishan plume head. The Sm/Yb ratio can be used to estimate the depth of melting because it is insensitive to the effect of fractional crystallization (e.g., McKenzie and O'Nions, 1991). The high Sm/Yb ratios of 2.25–3.12 and the depletion of HREE for the samples from Yanyuan indicate a magma origin involving smaller degrees of melting of a garnet-bearing mantle source. Taking account into the features of high La/Yb ratios and relatively low HREE concentration for these samples, we infer that the primitive magma for these rocks was originated from a garnet-bearing asthenospheric mantle source with relatively low degree of partial melting (Deniel, 1998; Xu et al., 2001) and associated with a mantle plume.

The mafic rocks from Huili and Panzhihua are compositionally comparable with the associated flood basalts in the Emeishan LIP. The intrusive and volcanic rocks of the Emeishan LIP both have the Sr–Nd isotopic signatures displaying an affinity to an OIB-like source (Fig. 7). These unequivocal similarities and also their close spatial and temporal association imply that they were the products of the same magmatic event at ~260 Ma.

The Ce/Pb, Nb/U and Th/La ratios for most samples are near or within the ranges for OIB (Sun and McDonough, 1989; Weaver, 1991), similar to those of high-Ti basalts in the Binchuan section, SW China (e.g., Xu et al., 2001; Xiao et al., 2004). The Nb/Th ratios are close to that estimated for OIB (Sun and McDonough, 1989). In addition, the OIB-like geochemical signatures are also supported by high LILE/LREE and LREE/HFSE ratios described above.
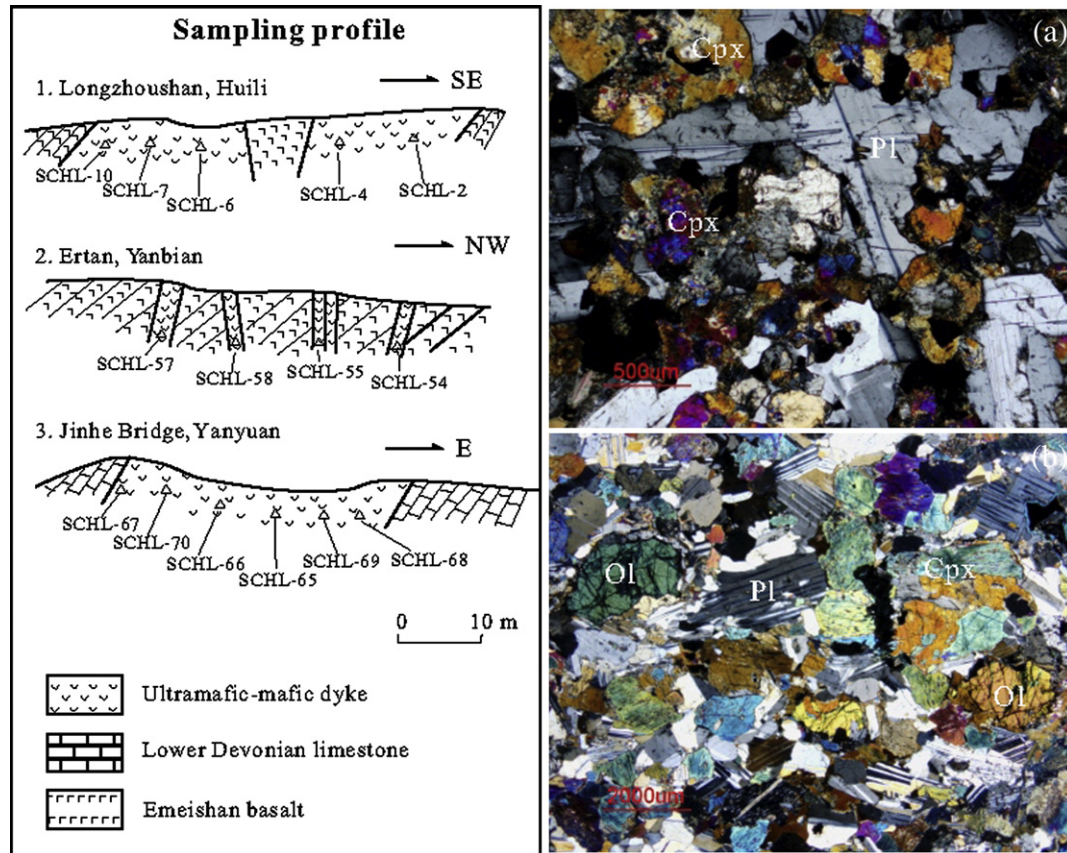
Fig. 8. Sampling profiles and photomicrographs of samples (a, b) from the Panxi mafic dykes, SW China. The photomicrographs were taken under cross-polarizer, transmission light. Pl, plagioclase; Cpx, clinopyroxene; Ol, olivine.

The (^{87}Sr/^{86}Sr)$_i$ ratios and $\varepsilon_{Nd}(t)$ data for these samples plot into the field of the Emeishan flood basalts, and extend from the OIB-like compositions toward the enriched quadrant (Fig. 7). This suggests a contribution from an enriched lithospheric component. Considering the fact that the western Yangtze Craton was an active continental margin during late Proterozoic ((Xiao et al., 2004) and references therein), it can be speculated that the subcontinental lithospheric mantle (SCLM) beneath this area had been modified by subducted slab-derived fluids (e.g., Ringwood, 1990; Hooper and Hawkesworth, 1993; Melluso et al., 2006). The previously metasomatized SCLM with arc-like geochemical signatures generated arc-type low-Ti magma when the Emeishan plume impinged onto the western Yangtze Craton (Xiao et al., 2004). However, this signature is not observed in the samples from the Panxi mafic dykes, although some samples from Huili and Panzhihua show weakly Nb–Ta depletion. In this regard, significant contribution of SCLM or subducted sediment-derived materials in the source region can probably be ruled out.

The generally depleted Sr–Nd isotopic signatures also support the proposal that the SCLM was not significantly involved in the formation and evolution of these mafic magmas. In addition, plume-derived melts generally have a low La/Ta ratio (8–15). This value will be much higher (generally >25) if the melts are modified by SCLM. In a different case, the melts contaminated by crustal materials have elevated La/Sm ratio

(>5) (Lassiter and DePaolo, 1997). According to these standard characteristics, we can infer that the samples from the Panxi region (with low La/Ta ratio, mostly <18) originated from a plume source, and the samples from Yanyuan (with relatively low La/Ta and La/Sm ratios, 13–15 and 2–3, respectively) experienced little contamination from SCLM or crustal materials. Furthermore, the samples from Yanyuan are depleted in incompatible element, and have the La/Nb ratios of 0.84–0.93, Th/Nb of 0.08–0.09, Zr/Nb of 6.67–9.02 and Ba/Nb of 9.07–15.69. This indicates the OIB-type geochemical signatures (Weaver, 1991), and is indistinguishable from those of the least contaminated picrites in the Emeishan LIP (Chung and Jahn, 1995).

The Sr–Nd isotopic compositions of the mafic dykes from Huili and Panzhihua can be interpreted to be result of variable crustal contamination of plume-derived magma during ascent and/or emplacement. This consideration is consistent with the high Th/Nb, Th/La and Rb/La ratios of these rocks and the correlation between their incompatible elements and elemental ratios (e.g., Nb vs. La/Nb) and between elemental ratios (e.g., La/Yb vs. Ce/Y) (Figs. 10 and 11).

6. Concluding remarks

The Emeishan LIP contains numerous mafic dykes and a variety of layered intrusions in addition to the voluminous
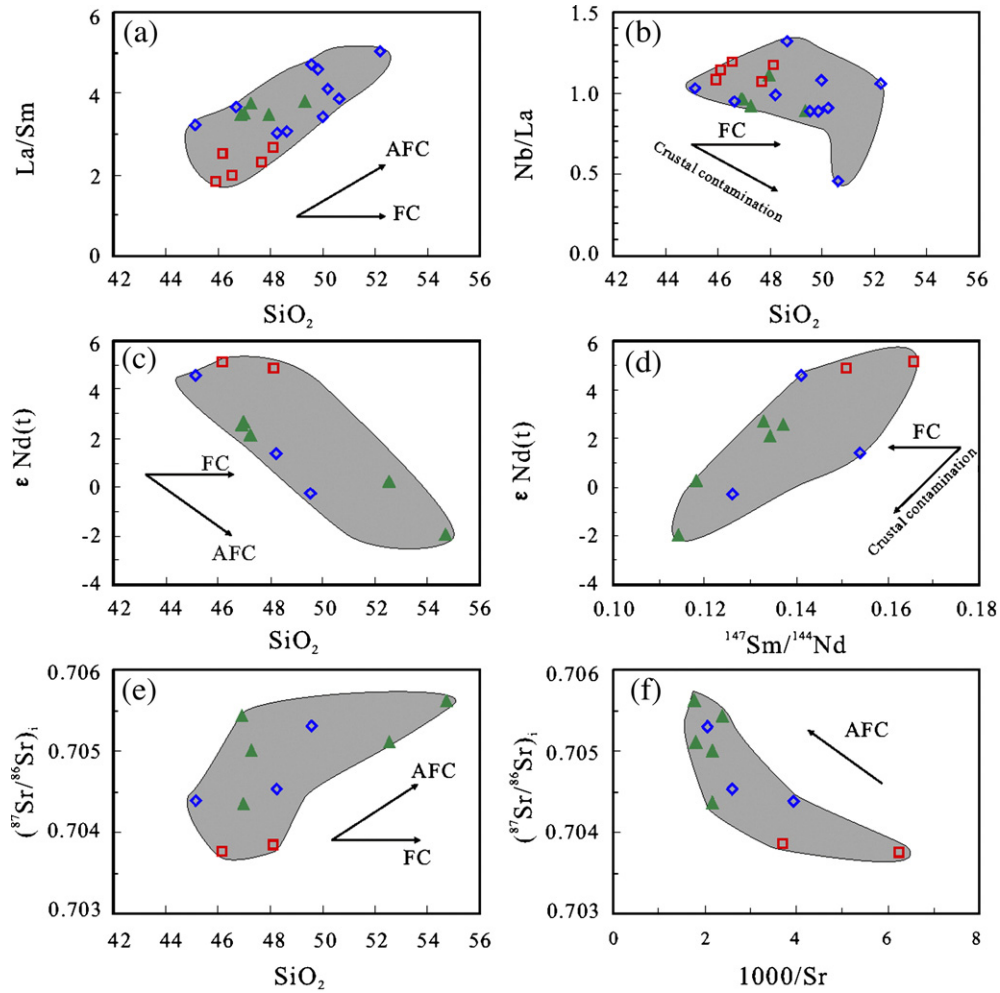
Fig. 9. Plots of the late Permian mafic dykes in the Panxi region, SW China. SiO$_2$ vs. La/Sm, Nb/La, $\varepsilon_{Nd}(t)$ and (^{87}Sr/^{86}Sr)$_i$, respectively (a–c, e); and ^{147}Sm/^{144}Nd vs. $\varepsilon_{Nd}(t)$ (d), 1/Sr vs. (^{87}Sr/^{86}Sr)$_i$ (f). FC, fractional crystallization; and AFC, assimilation and fractional crystallization. Symbols are the same as those in Fig. 2a.

Emeishan flood basalts. The mafic dykes in the Panxi region have ages identical to those of the associated volcanics and layered intrusions in Emeishan LIP, and they are compositionally and isotopically comparable with the Emeishan flood basalts. This indicates that these rocks were originated from melts produced by the same mantle plume at ~260 Ma.

It is proposed that the parental magmas to these mafic dykes were derived from a depleted mantle plume source with $\varepsilon_{Nd}(t) = \sim +6$ and (^{87}Sr/^{86}Sr)$_i = \sim 0.703$ in origin (within the garnet stability field), similar to those of the least contaminated Emeishan picrites and flood basalts (Fig. 7). The petrogenesis of the mafic dykes in the Panxi region is variably influenced by
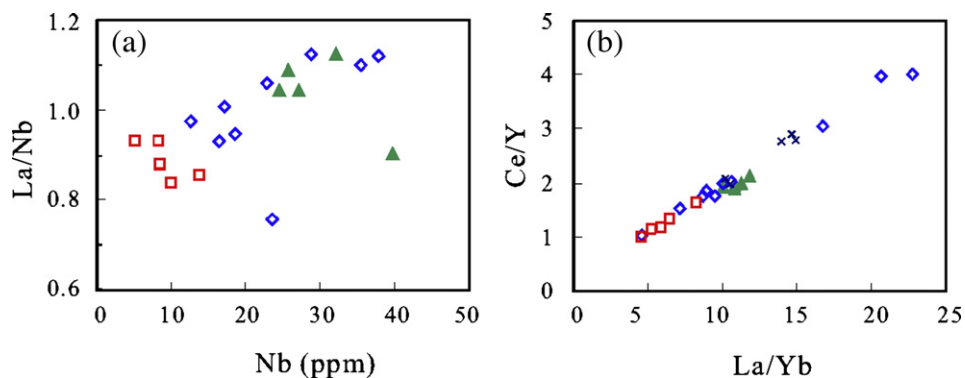

Fig. 10. Plots of Nb vs. La/Nb (a) and La/Yb vs. Ce/Y (b) for the Permian mafic dykes in the Panxi region, SW China. Symbols are the same as those in Fig. 2a.
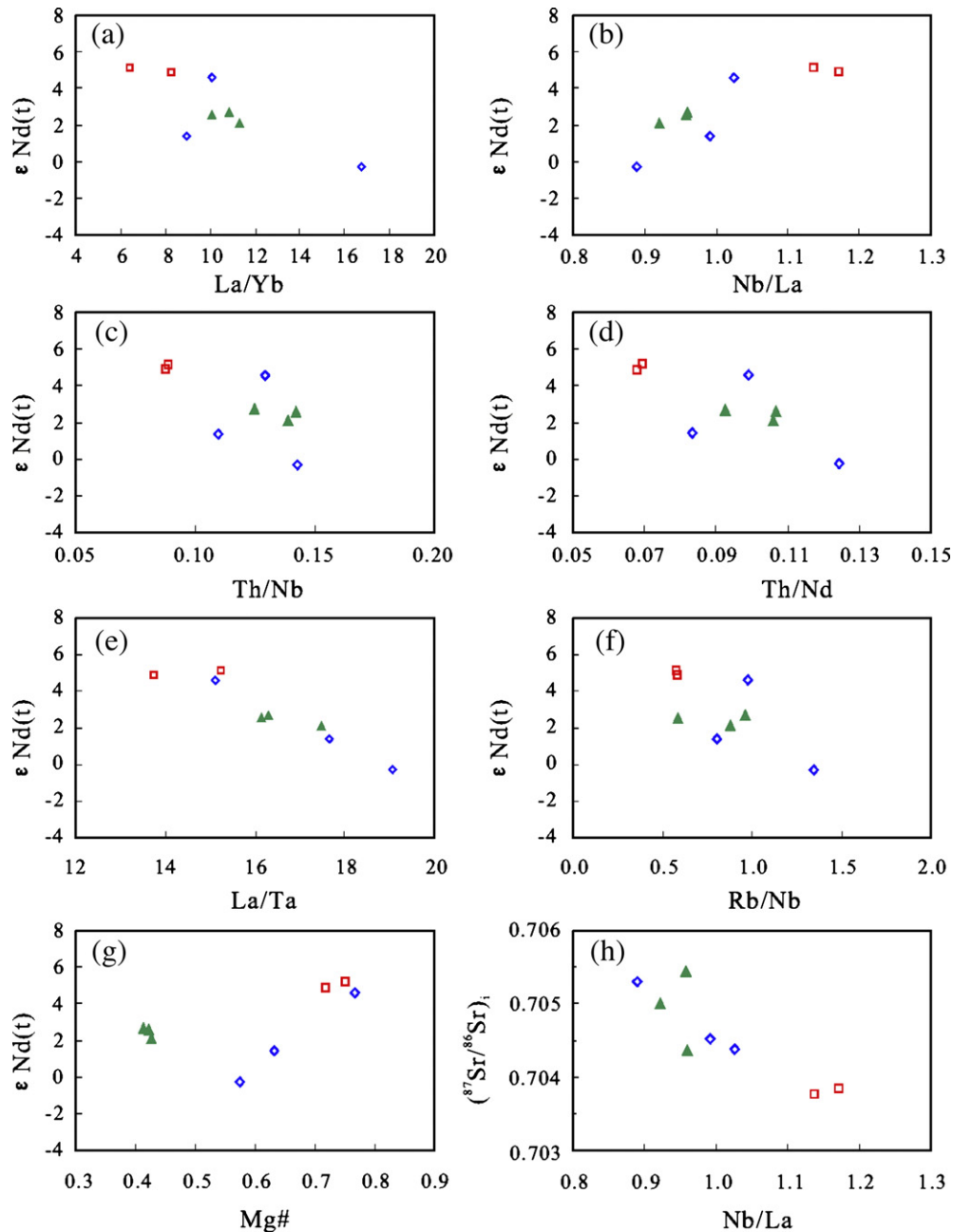
Fig. 11. Variations of $\varepsilon_{Nd}(t)$ with selected incompatible element ratios (a–f) and Mg# (g), and variation of $(^{87}Sr/^{86}Sr)_i$ with Nb/La (h) for the Permian mafic intrusive rocks in the Panxi region, SW China. Symbols are the same as those in Fig. 2a.

crustal contamination processes. The elemental and isotopic variations observed among these rocks reflect the involvement of these processes rather than a subcontinental lithospheric mantle (SCLM) source. The relatively undifferentiated Yanyuan gabbroic magma was least contaminated, likely representing a composition closer to primary melts. The melts were then subjected to extensive crystallization fractionation and different degrees of contamination by crustal materials, as reflected by elemental geochemistry and Sr–Nd isotopic features.

In summary, the temporal and spatial association and petrogenetic link between the mafic dykes in the Panxi region and the Emeishan basalts strongly suggest that these dykes are an integral part of the Emeishan LIP, and their intrusion is the products of the same magmatic event for this large igneous province, which formed a suite of flood basalts, ultramafic–mafic and intermediate-acidic alkaline intrusive rocks.

Guochun Zhao for their constructive reviews which substantially improved the scientific quality of the paper. Dr. Yanhua Zhang from CSIRO Exploration and Mining of Australia is thanked for improving the English.

References

Ali, J.R., Lo, C.-h., Thompson, G.M., Song, X., 2004. Emeishan Basalt Ar–Ar overprint ages define several tectonic events that affected the western Yangtze platform in the Mesozoic and Cenozoic. Journal of Asian Earth Sciences 23, 163–178.

Ali, J.R., Thompson, G.M., Song, X., Wang, Y., 2002. Emeishan Basalts (SW China) and the 'end-Guadalupian' crisis: magnetobiostratigraphic constraints. Journal of the Geological Society 159, 21–29.

Arndt, N., Chauvel, C., Czamanske, G., Fedorenko, V., 1998. Two mantle sources, two plumbing systems: tholeiitic and alkaline magmatism of the Maymecha River basin, Siberian flood volcanic province. Contributions to Mineralogy and Petrology 133, 297–313.

Arndt, N.T., Christensen, U., 1992. The role of lithospheric mantle in continental flood volcanism — thermal and geochemical constraints. Journal of Geophysical Research 97, 10967–10981.

Arndt, N.T., Czamanske, G.K., Wooden, J.L., Fedorenko, V.A., 1993. Mantle and crustal contributions to continental flood volcanism. Tectonophysics 223, 39–52.

Boven, A., Pasteels, P., Punzalan, L.E., Liu, J., Luo, X., Zhang, W., Guo, Z., Hertogen, J., 2002. $^{40}Ar/^{39}Ar$ geochronological constraints on the age and evolution of the Permo-Triassic Emeishan Volcanic Province, Southwest China. Journal of Asian Earth Sciences 20, 157–175.

Burchfiel, B.C., Chen, Z., Liu, Y., Royden, L.H., 1995. Tectonics of the Longmenshan and adjacent regions, central China. International Geology Review 37, 661–736.

Chung, S.-L., Jahn, B.-m., 1995. Plume–lithosphere interaction in generation of the Emeishan flood basalts at the Permian–Triassic boundary. Geology 23, 889–892.

Chung, S.L., Jahn, B.M., Lo, C.H., Cong, B., 1998. The Emeishan flood basalt in SW China: a mantle plume initiation model and its connection with continental breakup and mass extinction at the Permian–Triassic boundary. In: Flower, M.F.J., Chung, S.L., Lo, C.H., Lee, T.L. (Eds.), Mantle Dynamics and Plate Interactions in East Asia, pp. 47–58.

DePaolo, D.J., 1981. Trace element and isotopic effects of combined wallrock assimilation and fractional crystallization. Earth and Planetary Science Letters 53, 189–202.

Deniel, C., 1998. Geochemical and isotopic (Sr, Nd, Pb) evidence for plume–lithosphere interactions in the genesis of Grande Comore magmas (Indian Ocean). Chemical Geology 144, 281–303.

Fan, W.-M., Wang, Y.-J., Peng, T.-P., Miao, L.-C., Guo, F., 2004. Ar–Ar and U–Pb geochronology of Late Paleozoic basalts in western Guangxi and its constraints on the eruption age of Emeishan basalt magmatism. Chinese Science Bulletin 49, 2318–2327.

Fan, W., Zhang, C., Wang, Y., Guo, F., Peng, T., in press. Geochronology and geochemistry of Permian basalts in western Guangxi Province, Southwest China: evidence for plume-lithosphere interaction. Lithos. doi:10.1016/j.lithos.2007.09.019.

Gao, S., Ling, W., Qiu, Y., Lian, Z., Hartmann, G., Simon, K., 1999. Contrasting geochemical and Sm–Nd isotopic compositions of Archean metasediments from the Kongling high-grade terrain of the Yangtze craton: evidence for cratonic evolution and redistribution of REE during crustal anatexis. Geochimica et Cosmochimica Acta 63, 2071–2088.

Guo, F., Fan, W.M., Wang, Y.J., 2004. When did the Emeishan mantle plume activity start? Geochronological and geochemical evidence from ultramafic–mafic dykes in southwestern China. International Geology Review 46, 226–234.

He, B., Xu, Y.-G., Chung, S.-L., Xiao, L., Wang, Y., 2003. Sedimentary evidence for a rapid, kilometer-scale crustal doming prior to the eruption of the Emeishan flood basalts. Earth and Planetary Science Letters 213, 391–405.

He, B., Xu, Y.-G., Wang, Y.-M., Luo, Z.-Y., 2006. Sedimentation and lithofacies paleogeography in Southwestern China before and after the Emeishan flood volcanism: new insights into surface response to mantle plume activity. Journal of Geology 114, 117–132.

Hooper, P.R., Hawkesworth, C.J., 1993. Isotopic and geochemical constraints on the origin and evolution of the Columbia River Basalt. Journal of Petrology 34, 1203–1246.

Hou, G., Li, J., Yang, M., Yao, W., Wang, C., Wang, Y., 2008. Geochemical constraints on the tectonic environment of the Late Paleoproterozoic mafic dyke swarms in the North China Craton. Gondwana Research 13, 103–116.

Jin, Y., Shang, J., 2000. The Permian of China and its interregional correlation. In: Yin, H.F., Dickins, J.M., Shi, G.R., Tong, J. (Eds.), Permian–Triassic Evolution of Tethys and Western Circum-Pacific: Developments in Palaeontology and Stratigraphy. Elsevier Press, Amsterdam, pp. 71–98.

Lassiter, J.C., DePaolo, D.J., 1997. Plume/lithosphere interaction in the generation of continental and oceanic flood basalts: chemical and isotope constraints. In: Mahoney, J. (Ed.), Large Igneous Provinces: Continental, Oceanic, and Planetary Flood Volcanism. American Geophysical Union, pp. 335–355.

Lightfoot, P.C., Hawkesworth, C.J., Hergt, J., Naldrett, A.J., Gorbachev, N.S., Fedorenko, V.A., Doherty, W., 1993. Remobilisation of the continental lithosphere by a mantle plume: major-, trace-element, and Sr-, Nd-, and Pb-isotope evidence from picritic and tholeiitic lavas of the Noril'sk District, Siberian Trap, Russia. Contributions to Mineralogy and Petrology 114, 171–188.

Lightfoot, P.C., Naldrett, A.J., Gorbachev, N.S., Doherty, W., Fedorenko, V.A., 1990. Geochemistry of the Siberian Trap of the Noril'sk area, USSR, with implications for the relative contributions of crust and mantle to flood basalt magmatism. Contributions to Mineralogy and Petrology 104, 631–644.

Lin, J.Y., 1985. Spatial and temporal distribution of Emeishan basaltic rocks in the three southwestern provinces (Sichuan, Yunnan, and Guizhou) of China. Chinese Science Bulletin 30, 929–932 (in Chinese with English abstract).

Liu, D., Shen, F., Zhang, G., 1985. Layered intrusions of the Panxi Area, Sichuan Province. In: Zhang, Y. (Ed.), Contribution to Panzhihua–Xichang Rift, China. Geological publishing House, Beijing, pp. 85–118 (in Chinese).

Lo, C.-H., Chung, S.-L., Lee, T.-Y., Wu, G., 2002. Age of the Emeishan flood magmatism and relations to Permian–Triassic boundary events. Earth and Planetary Science Letters 198, 449–458.

Luo, Y.N., 1981. The characteristics of Ti-chromite mineralization in Xinjie layered ultramafic–mafic intrusion in Panzhihua area, China. Geochimica 10, 66–73 (in Chinese with English abstract).

Luo, Z., Xu, Y., He, B., Shi, Y., Huang, X., 2007. Geochronologic and petrochemical evidence for the genetic link between the Maomaogou nepheline syenites and the Emeishan large igneous province. Chinese Science Bulletin 52, 949–958.

Ma, C., Ehlers, C., Xu, C., Li, Z., Yang, K., 2000. The roots of the Dabieshan ultrahigh-pressure metamorphic terrane: constraints from geochemistry and Nd–Sr isotope systematics. Precambrian Research 102, 279–301.

Mahoney, J., 1988. Deccan Traps. In: Macdougall, J.D. (Ed.), Continental Flood Basalts. Kluwer Academic Publishers, Dordrecht, pp. 151–194.

McKenzie, D.A.N., O'Nions, R.K., 1991. Partial melt distributions from inversion of rare earth element concentrations. Journal of Petrology 32, 1021–1091.

Melluso, L., Mahoney, J.J., Dallai, L., 2006. Mantle sources and crustal input as recorded in high-Mg Deccan Traps basalts of Gujarat (India). Lithos 89, 259–274.

Naldrett, A.J., Lightfoot, P.C., Fedorenko, V., Doherty, W., Gorbachev, N.S., 1992. Geology and geochemistry of intrusions and flood basalts of the Noril'sk region, USSR, with implications for the origin of the Ni–Cu ores. Economic Geology 87, 975–1004.

Peng, P., Zhai, M.-G., Kusky, T.M., Zhao, T.-P., 2007. Nature of mantle source contributions and crystal differentiation in the petrogenesis of the 1.78 Ga mafic dykes in the central North China craton. Gondwana Research 12, 29–46.

PXGT, 1987. Metallogenetic Conditions and Geologic Characters of the Hongge Vanadic Titanomagnetite Deposit, Sichuan. Geological Publishing House, Beijing. 200 pp. (in Chinese).

Qi, L., Hu, J., Gregoire, D.C., 2000. Determination of trace elements in granites by inductively coupled plasma mass spectrometry. Talanta 51, 507–513.

Qiu, Y.M., Gao, S., McNaughton, N.J., Groves, D.I., Ling, W., 2000. First evidence of >3.2 Ga continental crust in the Yangtze craton of south China

and its implications for Archean crustal evolution and Phanerozoic tectonics. Geology 28, 11–14.

Ringwood, A.E., 1990. Slab–mantle interactions: 3. Petrogenesis of intraplate magmas and structure of the upper mantle. Chemical Geology 82, 187–207.

Rudnick, R.L., Gao, S., 2003. Composition of the continental crust. In: Holland, H.D., Turekian, K.K. (Eds.), Treatise on Geochemistry. Elsevier, pp. 1–64.

SBGMR, 1991. Regional Geology of Sichuan Province. Geological Publishing House, Beijing. (in Chinese).

Shellnutt, J.G., Zhou, M.-F., 2007. Permian peralkaline, peraluminous and metaluminous A-type granites in the Panxi district, SW China: their relationship to the Emeishan mantle plume. Chemical Geology 243, 286–316.

Shellnutt, J.G., Zhou, M.-F., Yan, D.-P., Wang, Y., in press. Longevity of the Permian Emeishan mantle-plume (SW China): 1 Ma, 8 Ma or 18 Ma? Geological Magazine.

Sheth, H.C., 2005. Were the Deccan flood basalts derived in part from ancient oceanic crust within the Indian continental lithosphere? Gondwana Research 8, 109–127.

Song, X., Hou, Z., Z., C., LU, J., Wang, Y., Zhang, C., Li, Y., 2001a. Geochemical characteristics and period of the Emei Igneous Province. Acta Geologica Sinica 75, 498–506.

Song, X.Y., Zhou, M.-F., Hou, Z.Q., Cao, Z., Wang, Y., Li, Y., 2001b. Geochemical constraints on the mantle source of the Upper Permian Emeishan continental flood basalts, southwestern China. International Geology Review 43.

Sun, S.s., McDonough, W.F., 1989. Chemical and isotopic systematics of oceanic basalts: implications for mantle composition and processes. In: Saunders, A.D., Norry, M.J. (Eds.), Magmatism in the Ocean Basins, pp. 313–345.

Taylor, S.R., McLennan, S.M., 1985. The Continental Crust: Its Composition and Evolution. United Kingdom, Oxford. Blackwell, p. 312.

Wang, Y., Fan, W., Zhao, G.-C., Ji, S., Peng, T., 2007. Zircon U–Pb geochronology of gneissic rocks in the Yunkai massif and its implications on the Caledonian event in the South China Block. Gondwana Research 12, 404–416.

Weaver, B.L., 1991. The origin of ocean island basalt end-member compositions: trace element and isotopic constraints. Earth and Planetary Science Letters 104, 381–397.

Winchester, J.A., Floyd, P.A., 1977. Geochemical discrimination of different magma series and their differentiation products using immobile elements. Chemical Geology 20, 325–343.

Xiao, L., Xu, Y.G., Mei, H.J., Zheng, Y.F., He, B., Pirajno, F., 2004. Distinct mantle sources of low-Ti and high-Ti basalts from the western Emeishan large igneous province, SW China: implications for plume–lithosphere interaction. Earth and Planetary Science Letters 228, 525–546.

Xu, Y.-G., He, B., Chung, S.-L., Menzies, M.A., Frey, F.A., 2004. Geologic, geochemical, and geophysical consequences of plume involvement in the Emeishan flood-basalt province. Geology 32, 917–920.

Xu, Y., Chung, S.-L., Jahn, B.-m., Wu, G., 2001. Petrologic and geochemical constraints on the petrogenesis of Permian–Triassic Emeishan flood basalts in southwestern China. Lithos 58, 145–168.

Yin, H.F., Huang, S., Zhang, K., Hansen, H.J., Yang, F., Ding, M., Bie, X., 1992. The effects of volcanism of the Permo-Triassic mass extinction in South China. In: Sweet, W.C., Yang, Z.Y., Dickins, J.M., Yin, H.F. (Eds.), Permo-Triassic Events in the Eastern Tethys: Stratigraphy, Classification, and Relations with the Western Tethys. Cambridge University Press, Cambridge, pp. 146–157.

Zhang, Z., LU, J., Tang, S., 1999. Sm–Nd ages of the Panxi layered basic–ultrabasic intrusions in Sichuan. Acta Geologica Sinica 73, 263–271.

Zhang, Z., Mahoney, J.J., Mao, J., Wang, F., 2006. Geochemistry of picritic and associated basalt flows of the Western Emeishan Flood Basalt Province, China. Journal of Petrology 47, 1997–2019.

Zhang, Z., Wang, F., Mahoney, J.J., 2004. Petrology, mineralogy, and geochemistry of the Emeishan Continental Flood Basalts, Southwestern China: evidence for activity of mantle plume. Acta Geologica Sinica 78, 40–51.

Zhang, Z.C., Wang, F.S., 2002. Geochemistry of two types of basalts of the Emeishan basaltic Province: evidence for mantle plume–lithosphere interaction. Acta Geologica Sinica 76, 138–147.

Zhong, H., Yao, Y., Hu, S.F., Zhou, X.H., Viljoen, M.J., Liu, B.-G., Luo, Y.-N., 2003. Trace-element and Sr–Nd isotopic geochemistry of the PGE-bearing Hongge layered intrusion, Southwestern China. International Geology Review 45, 371–382.

Zhong, H., Yao, Y., Prevec, S.A., Wilson, A.H., Viljoen, M.J., Viljoen, R.P., Liu, B.-G., Luo, Y.-N., 2004. Trace-element and Sr–Nd isotopic geochemistry of the PGE-bearing Xinjie layered intrusion in SW China. Chemical Geology 203, 237–252.

Zhong, H., Zhou, X.-H., Zhou, M.-F., Sun, M., Liu, B.-G., 2002. Platinum-group element geochemistry of the Hongge Fe–V–Ti deposit in the Pan–Xi area, southwestern China. Mineralium Deposita 37, 226–239.

Zhong, H., Zhu, W.-G., Chu, Z.-Y., He, D.-F., Song, X.-Y., 2007. Shrimp U–Pb zircon geochronology, geochemistry, and Nd–Sr isotopic study of contrasting granites in the Emeishan large igneous province, SW China. Chemical Geology 236, 112–133.

Zhou, M.-F., Malpas, J., Song, X.-Y., Robinson, P.T., Sun, M., Kennedy, A.K., Lesher, C.M., Keays, R.R., 2002. A temporal link between the Emeishan large igneous province (SW China) and the end-Guadalupian mass extinction. Earth and Planetary Science Letters 196, 113–122.

Zhou, M.-F., Robinson, P.T., Lesher, C.M., Keays, R.R., Zhang, C.-J., Malpas, J., 2005a. Geochemistry, petrogenesis and metallogenesis of the Panzhihua gabbroic layered intrusion and associated Fe–Ti–V oxide deposits, Sichuan Province, SW China. Journal of Petrology 46, 2253–2280.

Zhou, M.-F., Zhao, J.-H., Qi, L., Su, W., Hu, R., 2005b. Zircon U–Pb geochronology and elemental and Sr–Nd isotope geochemistry of Permian mafic rocks in the Funing area, SW China. Contributions to Mineralogy and Petrology 151, 1–19.

Zhou, J., Li, X.-H., Ge, W., Li, Z.-X., 2007. Age and origin of middle Neoproterozoic mafic magmatism in southern Yangtze Block and relevance to the break-up of Rodinia. Gondwana Research 12, 184–197.